PERFORMANCE REPORT ON THE AGS*

R.R. Adams, R.L. Cassel, C.H. Distenfeld, E.B. Forsyth, R.S. Frankel, W.E. Gefers, G.K. Green, J.J. Grisoli, A.W. Maschke, E.C. Raka, J. Spiro, A. van Steenbergen

Brookhaven National Laboratory, Upton, New York

(Presented by A. van Steenbergen)

I. Introduction

The scope of the AGS experimental program has grown steadily during recent years. An increasing demand for higher beam intensities simultaneously with multiple experimental set-ups has provided great impetus to the operational and technical development of the accelerator. Referring specifically to the period of approximately the last four years[1,2], in this time additional internal target stations have been developed, two fast external beam systems have been commissioned and significant progress has been made towards the installation of a slow external beam system.

Also, weekly average proton beam intensities have increased by a factor of 4-5, stimulating the development of sophisticated operational modes of simultaneous targeting and fast external beam usage. As a consequence, however, radiation levels around the AGS ring, radiation damage to components and exposure of personnel have become matters of continuing concern.

II. Accelerator Performance and Experimental Utilization

Mainly as a result of multiple turn injection, careful correction of injection fields (see below), in addition to an improvement of the linac beam intensity, together with the elimination of linac cavity beam loading, has it been possible to raise the AGS peak intensity to 2.2 10^{12} protons per pulse. The calculated incoherent space charge limit for the AGS is approximately 2.9 10^{12} protons/pulse, assuming a $\Delta\nu$ shift of 0.25 maximum. It is now recognized that $\Delta\nu$ could possibly be larger since traversal through, typically in the case of the AGS, the ν = 8 1/2 resonance is not disastrous and that for the AGS the incoherent space charge limit would be actually $\cong$ 4-5 10^{12} p/p. It is obvious that any improvements in maximum beam intensity, short of the scheduled incorporation of the 200 MeV linac, can only be small and would be the result of further improvements of many sub-systems. Typically, it is anticipated that with the incorporation of a higher brightness preinjector, scheduled for the spring 1968, and further sophistication of the linac beam loading compensation, higher beam intensities will be obtained.

Related to other space charge limitations, the vertical coherent ν value depression due to vacuum chamber image forces has been measured at injection in the AGS. Expressing the related space charge limit as $N_{sp} = 2K\nu_o(\Delta\nu)$, the value for K has been calculated and also deduced from ν value measurements. With this and assuming $\Delta\nu \cong \frac{1}{4}$, the coherent space charge limit would occur at $\cong$ 1.3 10^{13} pr/sec for the AGS. Further, a transverse vertical instability has also been observed and extensively investigated. A report on this (E. Raka) is presented elsewhere in the proceedings. Under normal operating conditions of good vacuum system pressure, it presents no intensity limit at the present time. Other possible charge related phenomena have been studied, typically beam blow-up immediately after injection, further reported elsewhere in the proceedings (A. van Steenbergen) and longitudinal blow-up during transition. Also, at the higher beam intensities beam-rf cavity interaction produces undesirable rebunching of the beam during the magnetic flat top. In this case, a totally unbunched beam is desired for a minimum ripple secondary beam spill from an internal target. Significant improvements could be made here by switching the "longitudinal bunch" from the stable fixed point of the rf bucket to the unstable fixed point, for about 1 msec, prior to starting the magnetic flat top. This "phase back" switching ($\cong$ 120°) stretches the longitudinal phase space occupation along the phase space separatrices and produces rapid debunching following rf turn off. This is further illustrated below (see also Fig. 6c).

Related to the peak intensities obtained in the AGS, improvements of component reliability, especially of the linear accelerator, the ring rf system and the vacuum system made it possible to achieve monthly average intensities of up to 1.4 10^{12} protons/pulse (Fig. 1) or of weekly average intensities in excess of this. The utilization of the scheduled operations time and AGS outage time is also shown in this figure. On an absolute time basis, during a recent one year period the AGS was scheduled for operations 83% of maximum possible running time of which 66% was used for high energy particle physics. This is further indicated in Table I, in which also is given the distribution of total accelerated protons amongst the various target stations and the fast external beam facility. A major share, i.e., $\cong$ 30% for the F9/F10 and $\cong$ 50% for the G9/G10 target stations, is used for counter experiments. The remainder is mainly used for target station F20A, serving a 30-in. bubble chamber; target station F20B, for a 31-in. bubble chamber and target station I10, either internal or external with the fast extraction system, serving the 80-in. bubble chamber. The target stations, in addition to external beam facilities, are further indicated in Fig. 2, in which an up-to-date view of the AGS complex is shown and also in Fig. 3, which illustrates a typical occupation of the West and East Experimental areas (summer 1967). As can be seen from this, it has been practicable to have set up 9-10 experiments at one time. Also it has been possible to operate actively with 5-6 experiments simultaneously during one machine cycle. A typical sequence of targeting and operation of the fast external beam system (July 1967) is given in the following table and further illustrated in Fig. 4.

Magn. Field	Target	Protons/Pulse	Spill	Experimental Utilization
rising	F20B	0.3 10^{11}	15 GeV, 75μsec	1.7 GeV/c, π^-, 31-in. B.C.
	F20A	1.2 10^{11}	22 - , 75 -	0.65 - , K^-, 30-in. B.C.
	I10 (Int.)	1.2 10^{11}	26 - , 100 -	8.0 - , π^-, 80-in. B.C.
	(Alternatively, I10 (Ext.), with fast external beam system)			
"flat top"	F9	1.0 10^{11}	28.5- , 500msec	20 - , π^-, Spark Chambers
	G10 (+4.7°)	9.0 10^{11}		20 - , $\pi^\pm$,$p^\pm$,$K^\pm$ Chambers
	G10 (+10.0°)			1 - , π^- Counters

Since the largest fraction of accelerated protons, (i.e., approximately 80%) is used during the flat-top mode, great emphasis has been placed on improving the length of the secondary beam spill and reducing its ripple content. Low frequency variations of the secondary beam spill are mainly related to the inherent regulation of the Motor-Generator rectifier combination, however, beam size and density distribution variations also do contribute to this. A servo loop, incorporating a plastic scintillation detector, which samples the secondary beam spill from the target, and the flat-top "phase back" rectifier control unit, is used to reduce the low frequency variations.

Spill modulation other than these slow variations are related directly to the magnet current ripple, i.e., sub-harmonics of the rectifier system and the rectifier fundamental harmonic. The sub-harmonics are due to mistiming of the individual rectifiers and a secondary control loop has been incorporated for "servo" timing control, related to the output voltage. The rectifier fundamental harmonic ripple content is reduced by means of an "active" ripple filter, whereby the inductance of a series saturable reactor is used as the regulating element of a shunt type ripple filter[3].

A block diagram of the present spill servo and magnet current ripple control is given in Fig. 5 and the effect of the various parameters on the secondary beam spill is given in Fig. 6. The latter figure illustrates (a) the effect of the fundamental ripple filter and the effect (b) of using the rf "phase back" technique, as mentioned before, in order to debunch the beam more effectively and more rapidly. In addition, the larger beam diameter (larger $\frac{\Delta p}{p}$) assist also in better spill control. The reduction of the magnet current variations and of the secondary beam spill variations can be summarized as follows:

	Magnet Current $(\frac{\Delta I}{I})$		Secondary beam spill variation (p-p) (Target Diameter 0.040 in.)	
	without corr.	with correction	without corr.	with correction
low freqs. (<10Hz)	0.015%	0.003%	up to 90%	<20%
60Hz ≤ Sub-harm.<720Hz	0.01%	0.003%	up to 60%	<20%
720Hz ≤ Rect.Fund.	0.03%	<0.0003%	up to 40%	<0.5%

III. Radiation Related Effects

As a result of the significantly increased number of accelerated protons per unit time, radiation exposure related effects have become a subject of constant attention. Radiation levels around the ring (averaged) have increased proportionately (Fig. 7b). Specifically radiation levels adjacent to target stations are significant, i.e., 100 hours after beam target interaction turn off, at two meters from the vacuum envelope in the medium plane, the radiation level, typically at the G10 target station, is still approximately 200 mrem/hr. These levels are high enough to demand careful scheduling of

*Work carried out under the auspices of the U.S. Atomic Energy Commission.

shutdown periods related to preshutdown operational modes. Curves, as given in Fig. 7a, illustrating the radiation decay near the G10 and F20 target stations are continuously updated and are used to schedule the required amount of target off time prior to a shutdown period, as related to estimated total personnel exposure for a particular scheduled component modification. Typically, a three week selected target turn off before shutdown is not unusual. The radiation exposure history of AGS personnel during recent years is given in Fig. 8, whereby the exposure data for 1967 are extrapolated on the basis of first half year data. The high exposure figures obtained during 1966 are to a certain extent specifically related to repeated repair periods in connection with organic "O" ring failures (radiation damaged), external beam component failure and target box modifications. Significant improvements have been made in these areas. Less versatile but quick interchangeable (throw away!) target boxes have been installed. Organic "O" rings have been replaced in all "hot" areas by metal rings. Second generation external beam components have been installed. As a result the overall radiation exposure of all personnel (and average exposure per person) begins to show at least a downward trend, notwithstanding that the total accelerated number of protons is still increasing. It is interesting to note (Fig. 8c) that modern high intensity proton accelerators may present personnel radiation exposure problems similar to (or worse than) that encountered with nuclear reactors.

With proton intensities in excess of 10^{12} protons per pulse, organic materials adjacent to the target sections have either failed or have been seriously damaged and required periodic replacment. Three typical organic materials, used in these areas, are indicated below with their expected life-times:

Material	Total Protons on Target	Total Dosage 2.5 m from Target	*Useful Life	Damage
coil insulation	$4\ 10^{18}$	$1.4\ 10^{9}$ (Rads)	1 yr.	Discoloration, delamination, lower surface resistivity.
organic "O" rings	$1\ 10^{18}$	$3.6\ 10^{8}$ -	½ yr.	Hardening, loss of resiliency.
water hoses	$2\ 10^{18}$	**$2.4\ 10^{8}$ -	½ yr.	Moderate to severe.

The main magnet coil insulation is composed of epoxy and polyester resins. After an exposure of 10^{9} rads, the coil insulation becomes discolored, delaminated and conductive. Even though no actual failures due to radiation damage have occurred, irradiated coils have been moved out of "hot" areas, since 1965, as a precautionary measure. A new coil insulation for the main magnet coils is now being used, which will withstand radiation doses an order of magnitude greater before radiation damage becomes critical, than can be tolerated with the present coil insulation. Three magnets, located near target stations, are now equipped with these coils.

The organic Viton "A" O-rings harden and lose resiliency. When installed, the rings have a hardness reading of 70-80 durometer, but after irradiation this figure increases by about a factor of two. These hardened gaskets have no longer the ability to provide a reliable vacuum seal. These rings have been replaced in the "hot" areas with Inconel-X rings coated with a few thousands of an inch of indium. The replacement rings fit the original "O" ring groove. The magnet water cooling hoses are made of neoprene rubber reinforced with rayon. Hose ruptures could be traced at least in part to the radiation damage. This problem has been solved by replacing the rubber hose, in the area of high radiation, with copper tubing.

IV. Accelerator Developments

Accelerator improvements and component modifications in recent years have been mainly related to linear accelerator, ring injection, beam manipulation and low field orbit corrections, and external beam systems.

The 750 kV preinjector now runs consistently with a well tested and reliable duoplasmatron ion source. An internal high field, high beam intensity, short column dc accelerator is nearing operational status. (This will be reported on elsewhere in the proceedings, Th. Sluyters, et. al.) It is planned to install this early 1968. The preinjector-linac beam transport has been modified to a 3-in. aperture beam matching system. The linac cavity proper has been modified by the replacement of the first set of eight drift tubes to provide for a larger linac acceptance. Also, in order to obtain improved beam loading compensation, the effective cavity length will be shortened by feeding the rf power at three locations along the length of the linac rather than the present single loop drive. The additional drive ports have already been installed. It is also intended here to re-arrange the high level rf system during the early part of 1968 to complete this modification. At present the high level rf drive system has already been modified with the incorporation of a 500 amp, 25 MW hard tube modulator, eliminating a line type modulator. This simplifies the problem of beam loading compensation and rf field regulation. This hard tube modulator will also be sufficient in conjunction with the planned three final FTH-515 stages, yielding a maximum rf power capability of 10.5 MW.

The linac-synchrotron transport and matching system has been modified (see Fig. 9) and includes a pulsed momentum analyzer and pulsed fast emittance measuring device, making continuous monitoring of E, ΔE, intensity and beam transverse phase space parameters possible. This, specifically, has improved the capability of the linear accelerator as a synhcrotron injector.

A most significant improvement of the AGS has been the installation of the multiple turn injection system. Injection takes place now by means of a thin septum dc inflector, which is offset by approximately 4.0 cm from the unperturbed equilibrium orbit. A shrinking $\lambda/2$ orbit perturbation is used during, typically, the first ten turns of injection, during which the accelerator is tuned more or less close to $\nu_x = 8.5$.

Further progress has been made with low field orbit correction elements. Specifically, correction of the horizontal gradient stopband at $\nu_x = 8\ 1/2$, by means of "(17θ)" quadrupole magnets and correction of the coupling gradient stopband $\nu_x + \nu_y = 17$ by means of "(17θ)" skew quadrupole magnets, have contributed to reducing beam losses shortly after injection in the AGS. For completeness sake the present arrangement of the AGS orbit perturbation elements have been given in Table II*.

Targeting has been improved by incorporation of high field orbit bumps, second generation rapid beam deflectors, servo controlled target movement mechanisms and sophisticated target injection and retraction controls.

In order to reduce further personnel radiation exposure, related specifically to target manipulation, an automatic target transfer mechanism has been installed, and this, in conjunction with an automatic cycling airlock, makes it possible to remove a target blade from the main AGS vacuum chamber and replace it with another held in an adjacent magazine. Eight different targets can be stored by the magazine of the device.

Related to accelerator control and monitoring a modest beginning has been made to incorporate an "on-line" computer facility. Especially as a monitoring device for the shortly to be installed slow external beam system (see below) it is expected to prove its value. As an element in the performance control of the AGS, progress is expected to be slow. In this respect, it is now not anticipated that the computer facility will expand rapidly over the present system, as schematically indicated in Fig. 10, especially since a future CDC-6600 (remote) computer link will permit extended computer capability without the necessity of expanding the local facility beyond the modest cost of the PDP-8 computers.

Related to the external beam facilities of the AGS, at the present time the AGS is equipped for fast beam extraction [5,6] at two locations (further details, see Fig. 2), i.e., for the external beam in the Southwest Experimental Area and for the external beam for the North Area, serving the 80-in. bubble chamber.

Probably the most important improvement made to the original system, is the redesign of the hydraulic ramming system used on the thin septum and ejector magnets. The new arrangement uses a variable delivery "swash" plate pump to deliver oil to the ram cylinder. The delivery rate of the pump is servo controlled, according to a program which minimizes shock forces during the magnet movement. The smoother stroke achieved by this change has produced a marked reduction in water leaks and fatigue type failures within the vacuum box.

When the "fast kicker" was installed, the magnet aperture was 2 in. x 5 in. As the AGS beam intensity has increased over the years, this magnet became a limiting aperture and recently it has been increased to 2 1/2 in. x 5 in. In order to maintain the same deflecting force, the characteristic impedance was changed from 4 ohms to 3 1/3 ohms by redesigning the pulse forming network and storage cables. At the same time, the performance of the kicker in the single bunch extraction mode was improved. A useful improvement in the operation was achieved by producing an orbit deformation during extraction, using a rapid beam deflector (RBD). The use of the RBD permits "parking" of the beam just prior to ejection, further away from the septum magnet and its associated fringe field, eliminating beam losses, caused otherwise by the many traversals through the fringe

*The following assumptions are made: Intensity $1\ 10^{12}$ p/p, $8\ 10^{18}$ p/yr, 50% on target.

**Estimate

*This is due, in part, to J. Herrera, who recently reviewed the existing low field orbit corrections in the AGS[4].

field. The RBD places the orbit close to the septum magnet only a few microseconds before the fast kicker is triggered.

During November of this year, it is intended to incorporate a slow external beam system with the AGS. The beam will be extracted using a third harmonic resonance excited by four sextupoles located symmetrically around the AGS ring[7,8]. Extraction will be done at the F10 location (Fig. 2) (replacing the present target station) by means of a thin septum magnet. This will be preceded at the F5 location by a hyper-thin septum magnet. The F5 and F10 magnets are powered by fast response current sources using series transistor banks as regulators. The F5 magnet supply is rated at 2,000 amperes, 24 volts, and the F10 magnet supply is rated at 7,500 amperes, 40 volts. Field variations due to ripple and thermal effects will be held within ±0.1%. All supplies are located in an equipment house, opposite the F10 location on the inside of the ring. It is connected to the ring tunnel by a 20-in. diameter pipe carrying bus bars and cables. The F5 magnet is a single piece edge cooled septum. The F10 magnet consists of three segments. The first segment is a two turn magnet, followed by two segments, each of which has three turns. The electroformed conductors are insulated with aluminum oxide, the core is iron nickel steel. Its $\int B.d\ell$ capability will be up to two Tesla-meters, for 600 milliseconds. Both septum magnets will not be rammed, however, the equilibrium orbit will be perturbed to bring the beam closer to the septum magnets prior to the excitation of the resonance blow-up. This will be done by means of eight presently installed backleg windings capable of producing three sequential $\lambda/2$ orbit bumps. Preliminary studies were done of the overall slow extraction process. In this case the beam was accelerated to full energy, with the radius "shifter" adjusted to bring the beam inside the radius where ν_x = 8 2/3, then the magnet "flat top" was started, followed by the excitation of sextupoles and orbit bump, subsequent to this the beam was allowed to spiral slowly outward by means of adjustment of the flat top slope, into the ν_x = 8 2/3 resonance and beam spill as a result of the resonant blow-up was observed at the F10 internal target station. Results so far have been satisfactory. A layout of the overall, initially to be installed, system is shown in Fig. 11. As shown, the option will exist to study all beam properties in an analysis channel, prior to switching the beam into the primary beam experimental channel. This permits a wider choice of beam analysis instrumentation (typically, for emittance measurements) and also will eliminate harmful irradiation with an improperly "tuned" beam of all components leading to the external target station. The bore of the experimental channel is three inches, the analysis channel has a minimum bore of four inches, widening to eight inches.

Upstream of the bending magnet, as shown, vertical and horizontal steering magnets will be placed. These are ferrite magnets with a useful response up to 1 kHz. The deflection will be ± 1 milliradian for the horizontal "steerer" and ± 1/4 milliradians for the vertical steerer. Adjacent to these magnets are two horizontal deflection magnets for the purpose of providing a sinusoidal motion to the beam. A low frequency (60 Hz) magnet is used in conjunction with a wire target to make emittance measurements of the extracted beam. A high frequency (10 kHz) magnet is used to derive phase information for the servo system, which guides the beam onto the target using the horizontal steerer. Initially, beam current monitoring will be done by means of a secondary emission chamber and a gas scintillation chamber. The signals will be used for spill modulation analysis and to normalize the steering servo error signals. Various targets and flags will be incorporated for further beam set-up analysis.

Acknowledgments

This paper summarizes the work of many of the AGS staff who assisted in the very pronounced improvements which have been made. The authors wish to acknowledge their efforts categorically.

Further, specific credit is due to A. Watts, for the results contained in Fig. 4, similarly, E. Gill for those presented in Fig. 6 and J. Davis and others of the AGS Health Physics Group, who assisted in providing the data contained in Figs. 7 and 8.

References

1. G.K. Green, "AGS Performance and Plans," International Conference on High Energy Accelerators, Proceedings, Dubna, 1963.

2. R.R. Adams, E.B. Forsyth, W. Gefers, G.K. Green, H.J. Halama, A.W. Maschke, M. Plotkin, J. Spiro, "Multiple Experimental Operation at the AGS," International Conference on High Energy Accelerators, Proceedings, Dubna, 1963.

3. R. Cassel, H. Halama, "Electronic Ripple Filter for the Brookhaven AGS," Nuclear Instruments and Methods 42, 1966, 157.

4. J.C. Herrera, C. Lasky, M. Month, "AGS Low Field Correction Elements," IEEE Transactions on Nuclear Science, June 1967, NS-14, 3, 425.

5. G.K. Green, "External Beam - Part I," BNL Accelerator Department Internal Report GKG-6, October 10, 1962.

6. E.B. Forsyth, C. Lasky, "The Fast Beam Extraction System of the Alternating Gradient Synchrotron," BNL Report BNL 910 (T 373), March 10, 1965.

7. M.Q. Barton, "Preliminary Work on the Slow Extracted Proton Beam," BNL Accelerator Department Internal Report AADD 86, January 20, 1965.

8. M.Q. Barton, J. Faure, "Improved Calculations of Properties of the Slow Extracted Beam," BNL Accelerator Department Internal Report AADD 131, February 3, 1967.

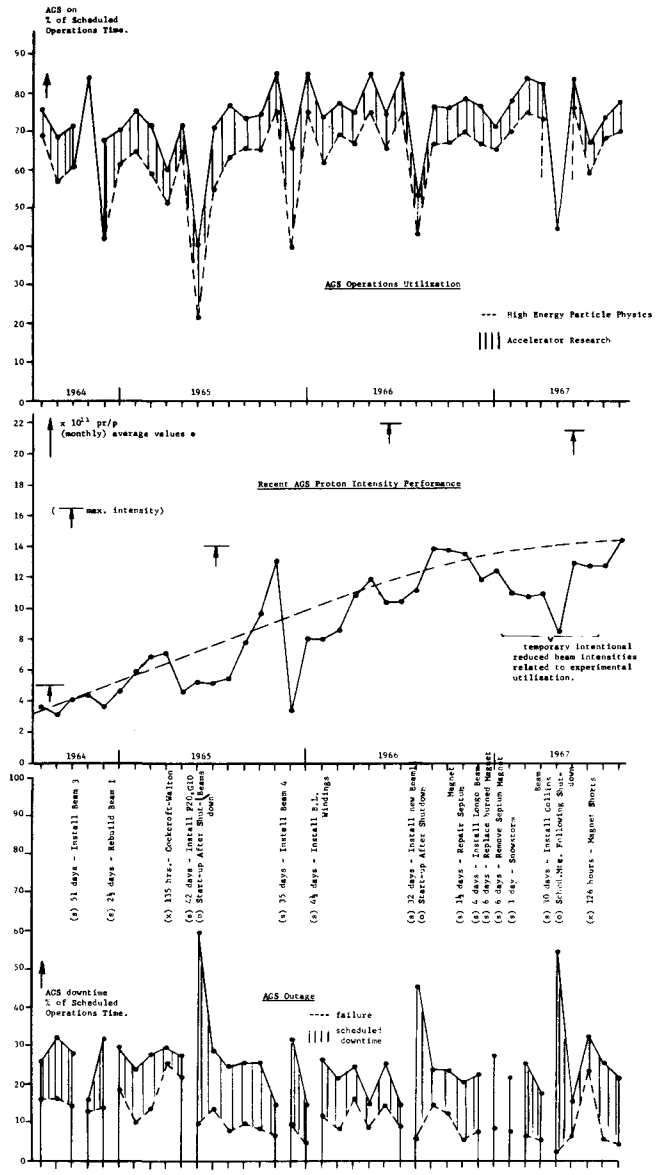

Fig. 1

AGS Performance; Utilization, Intensity, Outage.

Typical AGS Utilization ('66-'67). Sum of enclosed areas represents scheduled operation time. Percentages refer to scheduled time, which is 83% of maximum possible running time.

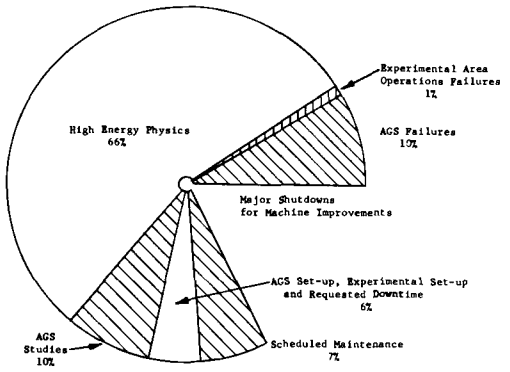

Distribution of Accelerated Protons (Same Period)

Internal Targets, External Beams		% of Accel. Protons	Protons on Target
F9/F10*	internal target, slow spill, flat top	31	25.3×10^{17}
F20A	internal target, fast spill, RBD	9.4	7.7×10^{17}
F20B	internal target, fast spill, RBD	0.1	0.1×10^{17}
G9/G10	internal target, slow spill, flat top	48	39.2×10^{17}
G20	internal target, radio-chemistry	0	0.0
H10	internal target, special use, mainly radiation studies	0.2	0.2×10^{17}
I10	internal target, fast spill, RBD	1.3	1.1×10^{17}
I10	external beam, fast spill	9.7	7.9×10^{17}
B10	external beam, fast spill	0	0.0
		Total Protons on Target	$81.5 \quad 10^{17}$

*Letters indicate locations of the twelve "superperiods" of the AGS.

Table I

Table I Typical Operations Utilization and Distribution of Protons.

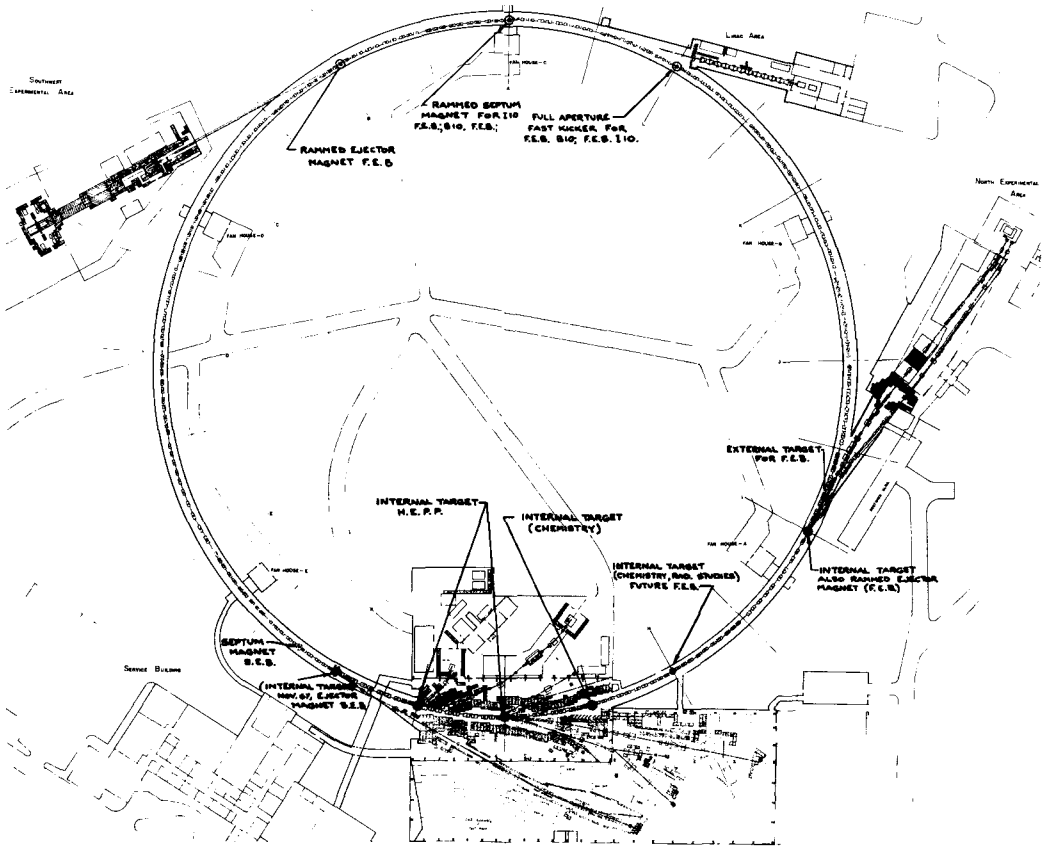

Fig. 2 Present AGS General Layout of Target Stations and External Beams.

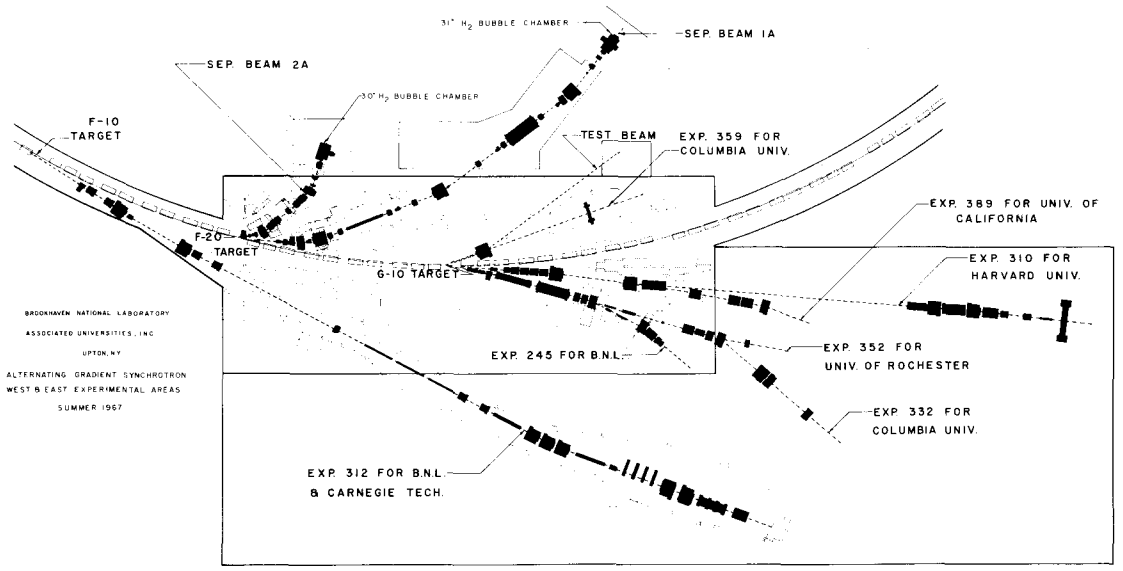

Fig. 3

Occupation West and East Experimental Areas, Summer 1967.

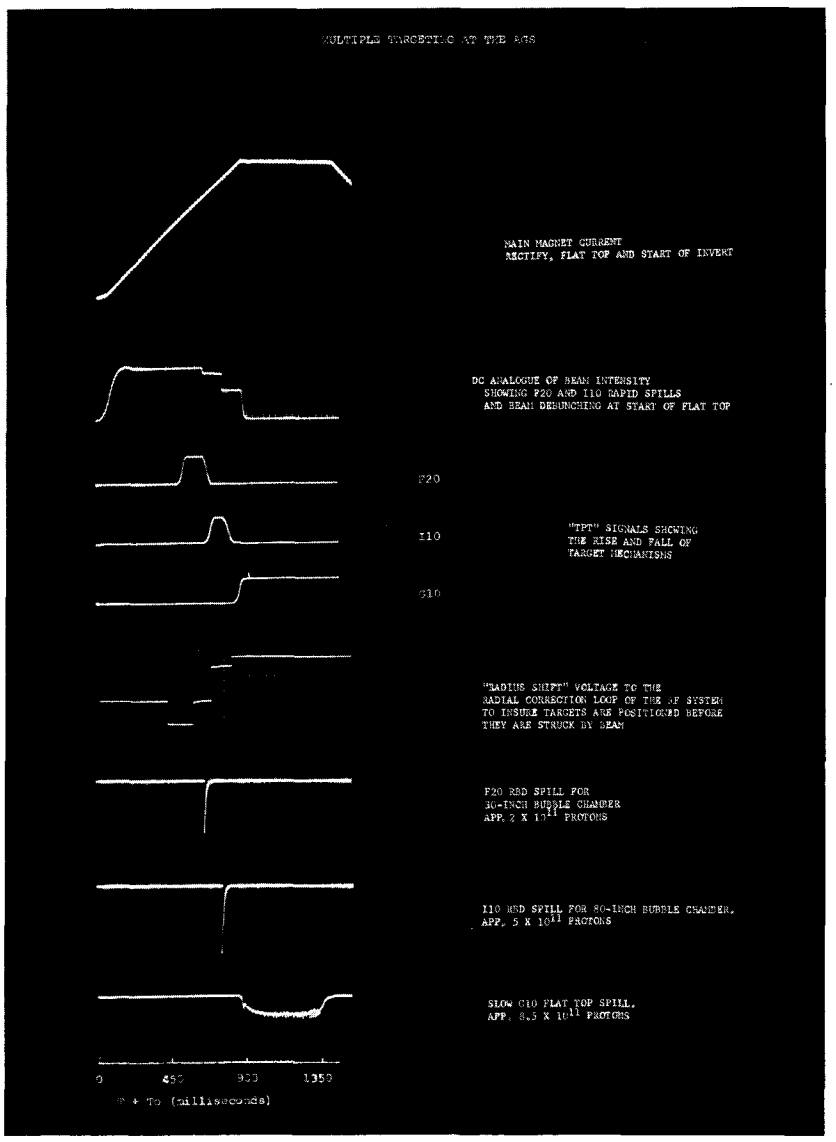

Fig. 4

Multiple Targeting, Typical Operational Mode.

Block diagram of magnet current "spill servo",
secondary control loop and ripple filter.

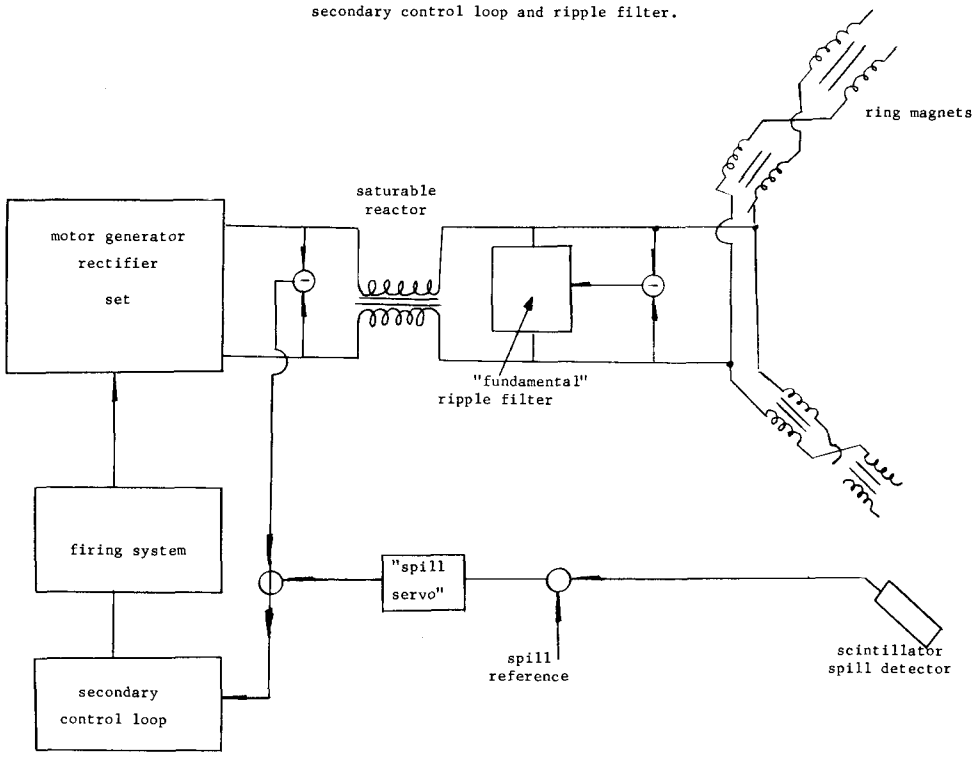

Fig. 5

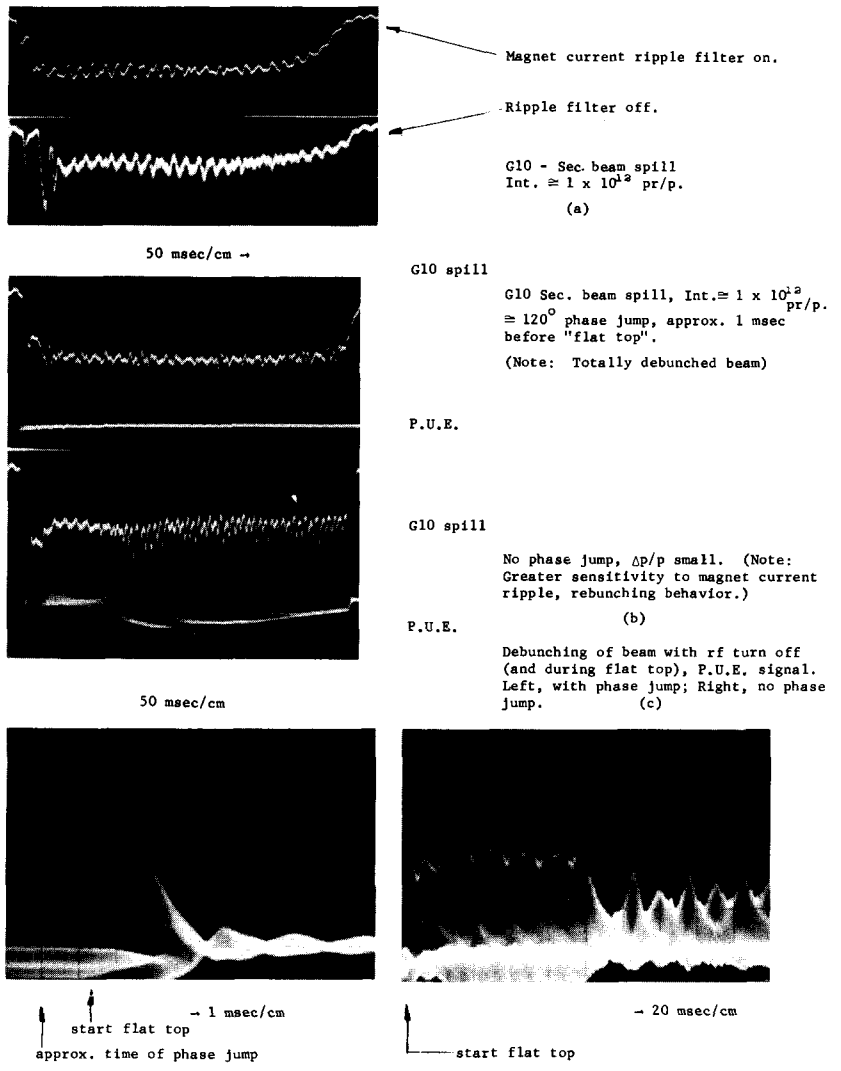

Fig. 6 G10 Secondary Beam Spill, Effect of Ripple Filter and "Phase Back" Technique.

Fig. 5 Block Diagram of Magnet Current "Spill Servo," Secondary Control Loop and Ripple Filter.

Fig. 6 G10 Secondary Beam Spill, Effect of Ripple Filter and "Phase Back" Technique.

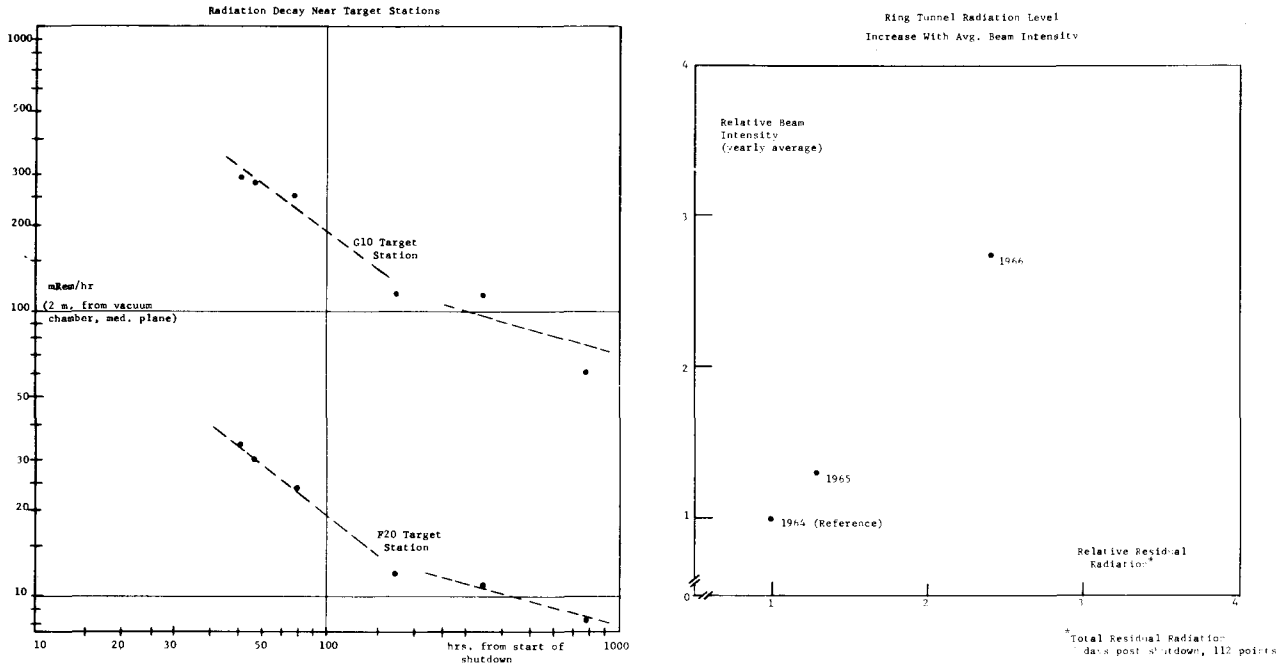

Fig. 7

Radiation Decay Near Target Stations and Increase of Ring Tunnel Radiation Levels with Intensity.

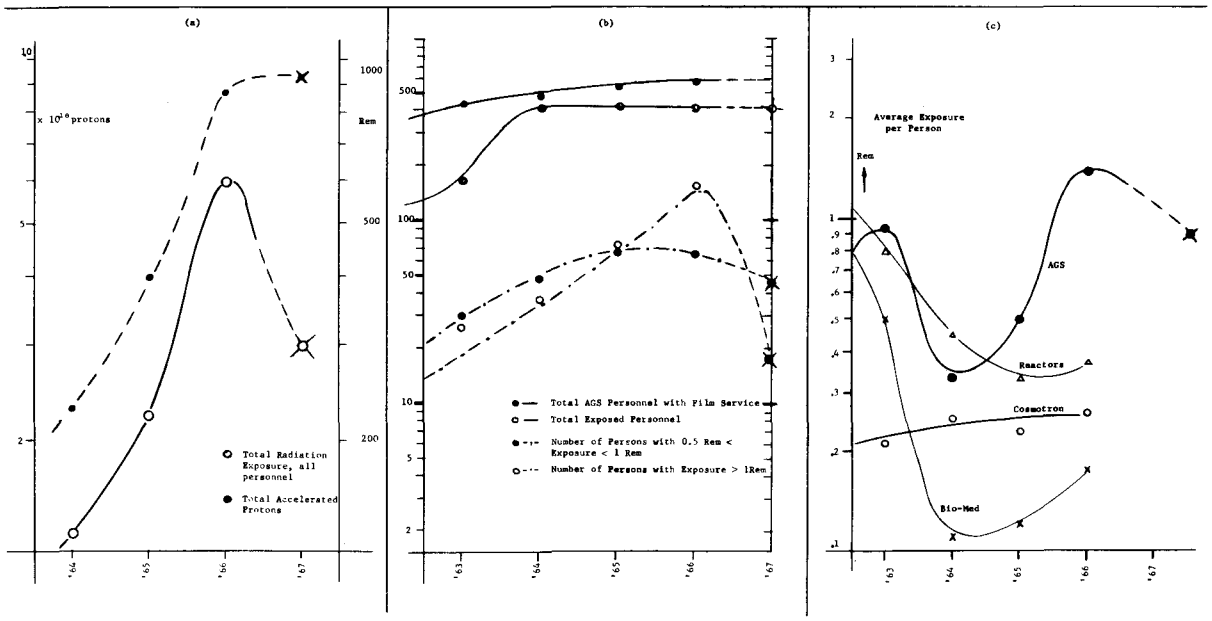

Fig. 8

AGS Personnel Radiation Exposure History.

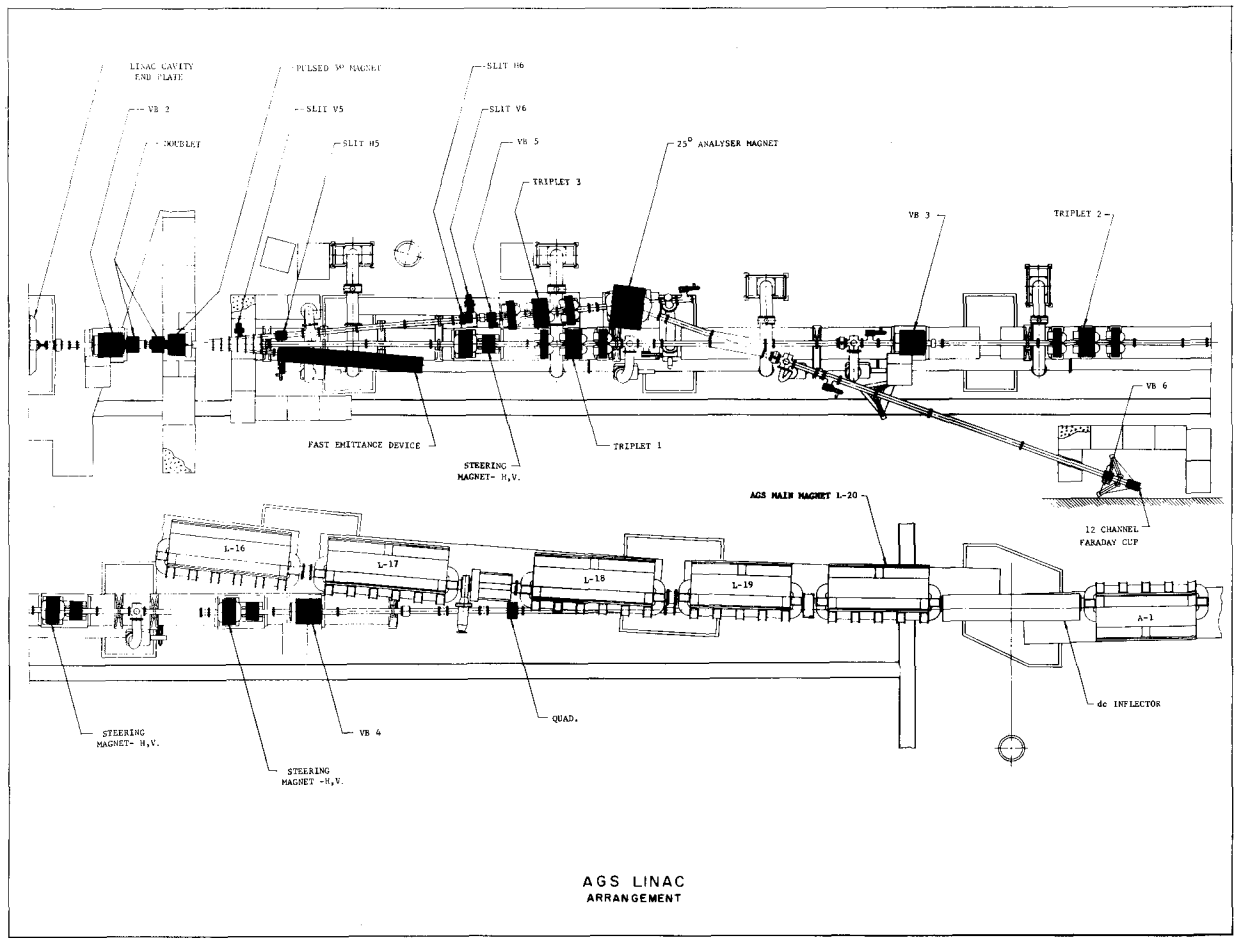

AGS LINAC
ARRANGEMENT

Fig. 9

Linac-AGS Beam Transport, Matching and Analysis System.

Present Arrangement of AGS Orbit Perturbation Elements

	Component	Location	Effect
Gradient	High Field Quad.	St. Sect. 3, 17 (all superper.)	ν value control. (ν value correction for fixed radius operation.)
	(17θ) Quad.	C17,F17,I17,L17	Corrects for the horizontal gradient stopband at $\nu = 8\frac{1}{2}$.
	Backleg Windings (low field)	All magnets	Not used
	Backleg Windings (high field)	E6,E7,E20,F1,F14, F15,G8,G9	High field orbit deflection for slow beam, total gradient perturbation = 0.
	Special Quad.	C5	ν value perturbation for slow external beam.
Field	Dipole "Pancakes" sin 12θ	Even 2' st.sects. (all superper.)	Corrects the twelfth harmonic vertical distortion of the equilibrium orbit produced by the earth's magnetic field.
	Dipole "Pancakes" sin 9θ, cos 9θ sin 8θ, cos 8θ, resp.	8,18,2,12,... 2,12,8,18,... A6,A19,B1,B14,C1, C9,... A1,A11,B9,B11,C4, C6,..., resp.	Corrects for the eighth and ninth harmonic vertical distortion in the equilibrium orbit due to perturbing fields.
	Backleg Windings (low field)	All magnets	Horizontal orbit corrections, not used.
	Backleg Windings (high field)	E6,E7,E20,F1,F14, F15,G8,G9	High field orbit deflection for slow external beam (3 x λ/2).
Gradient Coupling	"Twist" Quad. (bucked pancake)	Set of 8θ, 9θ dipole pancakes	This corrects for the horizontal to vertical coupling due principally to the earth's magnetic field.
	(17θ) Skew Quad.	B15,E15,H15,K15 (+ + - -)	Corrects for coupling gradient stopband at $\nu_h + \nu_v = 17$.
Second Order Correction	Sextupole (high field)	St. Sect. 13, 7 (all superper.)	Coherence damping. Control $\nu = f(r)$ behavior for SEB.
	Sextupole (high field)	St. Sect. B5,E5,H5,K5	$\nu = 8\ 2/3$ resonant slow extraction driving force.
	Sextupole (high field)	A5,D5,G5,J5	Not used

Table II

Table II Present Arrangement of AGS Orbit Perturbation Elements.

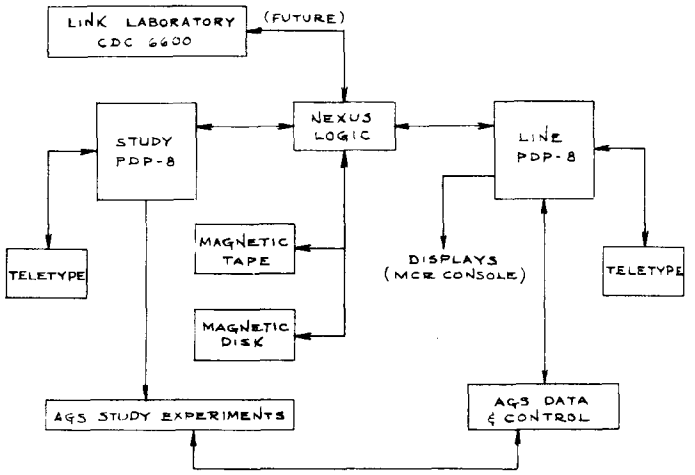

AGS "ON LINE" COMPUTER COMPLEX

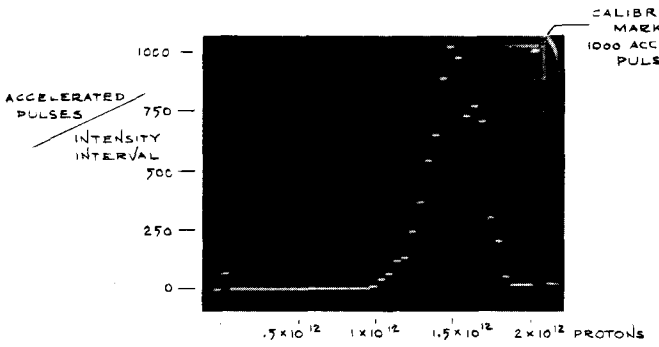

A Computer Generated AGS Beam Intensity Frequency Distribution

Fig. 10

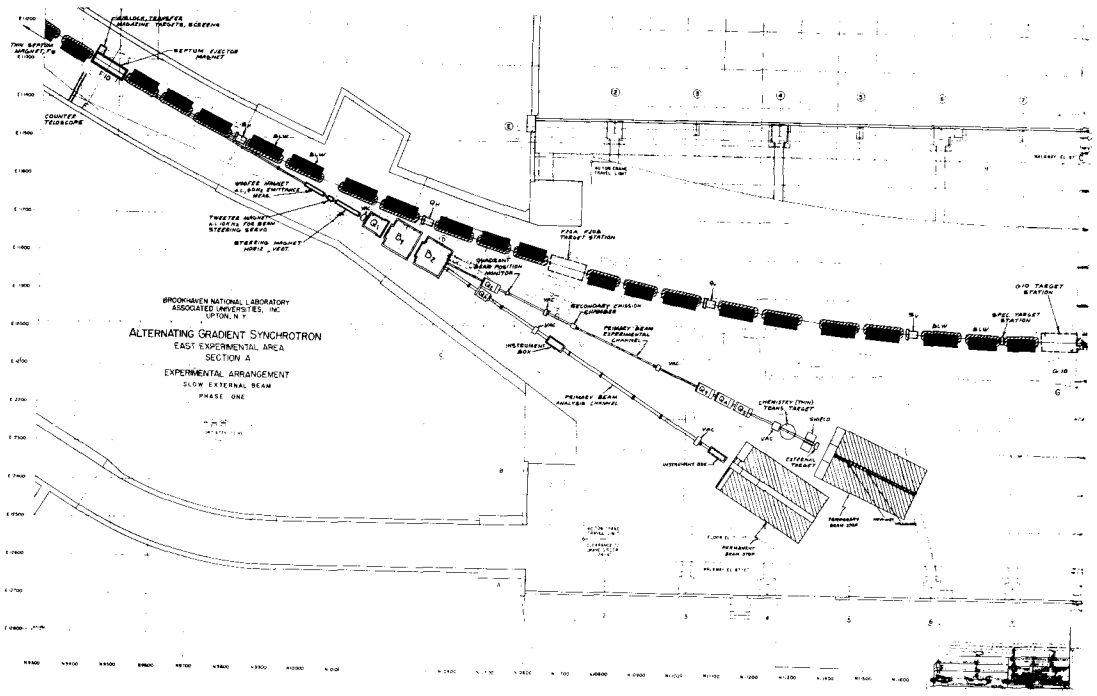

Fig. 11 Initial Layout of the Slow External Beam Facility (to be installed November 1967).

Fig. 10 AGS "On-Line" Computer Arrangement.

Fig. 11 Initial Layout of the Slow External Beam Facility (to be installed November 1967).